Shock and Vibration 20 (2013) 199–211
DOI 10.3233/SAV-2012-00738
IOS Press

Topology optimization of passive constrained layer damping with partial coverage on plate

Weiguang Zheng[a,b], Yingfeng Lei[b,c], Shande Li[a] and Qibai Huang[a,b,*]
[a]*State Key Laboratory of Digital Manufacturing Equipment and Technology, Huazhong University of Science and Technology, Wuhan, China*
[b]*State Key Lab of Vehicle NVH and Safety Technology, Chongqing, China*
[c]*Changan Automobile Engineering Institute, Chongqing, China*

Received 12 March 2012
Revised 18 June 2012

Abstract. The potential of using topology optimization as a tool to optimize the passive constrained layer damping (PCLD) layouts with partial coverage on flat plates is investigated. The objective function is defined as a combination of several modal loss factors solved by finite element-modal strain energy (FE-MSE) method. An interface finite element is introduced to modeling the viscoelastic core of PCLD patch to save the computational space and time in the optimization procedure. Solid isotropic material with penalization (SIMP) method is used as the material interpolation scheme and the parameters are well selected to avoid local pseudo modes. Then, the method of moving asymptote (MMA) is employed as an optimizer to search the optimal topologies of PCLD patch on plates. Applications of two flat plates with different shapes have been applied to demonstrate the validation of the proposed approach. The results show that the objective function is in a steady convergence process and the damping effect of the plates can be enhanced by the optimized PCLD layouts.

Keywords: Topology optimization, passive constrained layer damping, modal loss factor

1. Introduction

Constrained layer damping (CLD) is recognized as an effective means for damping out the resonant vibrations and noise radiations of thin-walled structures [1]. The vibratory energy is dissipated due to shear strains in the viscoealstic layer of CLD patch. When the base structure vibrates in bending, the stiff constraining layer will force the viscoelastic materials (VEMs) to deform in shear due to the differences between the displacements of the base structure and the constraining layer, resulting in conversion of structural vibration energy into heat. The CLD treatments provide considerably more damping effect than the unconstrained ones in spite of adding extra weight of the constraining layer. Earlier works mainly focused on passive constrained layer damping (PCLD) treatments whose constraining layers are made of passive materials (e.g., metal). The original contributions to the PCLD technology are from Kerwin [2] who developed a simplified theory to calculate the loss factor of a plate with PCLD treatment. After that, different formulations and techniques have been published for modeling and predicting the energy dissipation of the viscoelastic core layer when the PCLD treated structure is vibrating [3–5]. Recently, active constrained layer damping (ACLD) [6,7] technology has begun to receive more attention and shown its significant advantage of attenuating low frequency vibrations. The ACLD configuration uses an active piezoelectric layer to replace the traditional passive constraining layer to enhance the energy dissipation of the damping. However, ACLD treatment

*Corresponding author: Qibai Huang, School of Mechanical Science and Engineering, Huazhong University of Science and Technology, Wuhan 430074, China. Tel.: +86 27 87557664; Fax: +86 27 87544175; E-mail: qbhuang@mail.hust.edu.cn.

ISSN 1070-9622/13/$27.50

suffers form its high cost and complexity. Therefore, PCLD treatment is more applicable than ACLD treatment in traditional industry. Nowadays, it is a very common practice for automakers to add PCLD patches to the structures like oil pans, front covers, valve covers, etc. to solve resonant noise and vibration problems.

As the weights often play a key role in the performance and cost in the products, the efficient use of the PCLD treatments is a main topic concerned by design engineers. Especially, in low frequencies, the placement of the PCLD patch would have significant effect on the damping of the structure due to the low structural modal density in this frequency range. During recent years, extensive efforts have been exerted to optimize the damping treatments for better damping effects through the use of various structural optimization methodologies, resulting in a large number of studies in the field. Plunkett and Lee [8] presented a method to increase the energy dissipation in the structure by placing segmented constraining layers of optimum length on an unconstrained beam. Lall et al. [9] carried out multi-parameter optimum design studies for a sandwich plate with constrained viscoelastic core. Design variables were chosen as material densities, thicknesses, and temperature, with objective functions as modal loss factor and displacement response. Marcelin et al. [10] used finite element method (FEM) and genetic algorithm (GA) to maximize the damping factor for partially covered beam. The design variables were the dimensions and locations of the patches. Zheng et al. [11,12] studied the optimal layout of PCLD on beams for minimization vibration energy and sound radiation based on analytical models using GA with penalty functions for constraints.

All of these studies above performed shape or size optimization are at the level of macroscopic design, using a macroscopic definition of geometry given by for example dimensions or boundaries. One of the limitations of these conventional shape or size optimizations by boundary variations is that the topology of structure is fixed during the iterative design process. A very interesting idea is proposed by Alvelid [13] who suggested a shape optimization method by adding the PCLD to the base structure piece by piece at permissible positions in a mosaique manner with the objective function as the square of the surface velocity. Though the shape is not limited in the optimization procedure, the optimized results may not be the best in a global perspective as the adding manner of PCLD element is not very flexible. Thus, an introduction of a new method that can yield the optimal topology and shape of a structure is needed. The subject can be known as topology optimization based on micromechanics which are suitable for shape or sizing problems. The topology optimization can be thought of as how to redistribute the material in order to minimize/maximize the objective function for a given set of loads and boundary conditions. The topology optimization method for continuum structures first appeared in the literature about twenty years ago by Bendsøe and Kikuchi [14]. Structural topology optimization has been an extremely active area of research since then [15]. The method applied to the viscoelastic materials was initially suggested by Yi et al. [16] who used homogenization method of topology optimization to maximize the damping characteristics of viscoelastic composites. Lumsdaine [17] extended the homogenization method to determine the optimal topologies for viscoelastic layer along its thickness of a PCLD treated beam with the aim of maximize the system loss factor. Mohammed [18] dealt with the optimal distribution for viscoelastic materials on sandwiched damping beams or plates using inverse homogenization method to maximize the modal loss factors. Recently, Ling et al. [19] extended Mohanmmed's work to optimize the viscoelastic materials distribution in ACLD using solid isotropic material with penalization (SIMP) model [20] solved by method of moving asymptote (MMA) approach [21]. However, work on topology optimization of PCLD patches partially added on a base structure has not been carried out up to now. Only optimizing the viscoelastic materials [18,19] can't get effective weight reduction due to the fact that viscoelastic layer of PCLD patch is often low in density and small in thickness.

One of the main difficulties in the topology optimization of PCLD patches is that FEM is always needed. While the dynamic solution procedure of the structure including viscoelastic materials using FEM is very time consuming due to the complex properties of the viscoelastic materials. In the late 1970s, FEM was firstly introduced by Lu et al. [22] as a general method for solving problems of sandwich plates. Johnson and Kienholz [23] estimated the modal damping ratios of three-layer laminates by means of the finite element-modal strain energy (FE-MSE) method. The proposed method was very useful for large-scale problems because of less computation time needed to solve real undamped eigenvalue problems. Recently, FE-based commercial codes, such as ANSYS, ABAQUS, NASTRAN, etc., have been available to the market for modeling PCLD treatments. Though it is convenient to model complex structural with general boundary conditions by FEM, the mesh has to be very dense to satisfy the requirement of element aspect ratio because of small thicknesses of viscoelastic and constraining layers, which results in extremely large model and very expensive computation, especially in optimization problems. Some efforts have been done

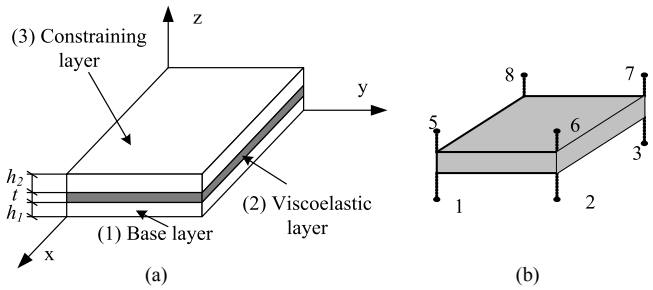

Fig. 1. Schematic of the model. (a) PCLD element; (b) interface element for viscoelastic core.

to overcome the weakness of conventional FEM. Zhang and Sainsbury [24] applied the Galerkin element method (GEM) to the vibration analysis of damped sandwich structures for the purpose of improving the convergence and accuracy of the FEM. Alvelid and Enelund [25] developed a general interface finite element that can directly couple together the shell elements of base and constraining layers. The notion is adopted in our present work and an eight node interface finite element model is developed. The number of the elements of the structure can be largely reduced by the proposed element, which is attractive for the topology optimization using SIMP method as the number of the design variables is the same as the number of elements.

The main goal of this paper is to investigate the use of structural topology optimization as a tool to optimize the PCLD treatments with partial coverage in order to enhance the energy dissipation mechanism and improve the damping characteristics of vibrating plates. An interface finite element is introduced to modeling the viscoelastic layer of PCLD treatment and FE-MSE method is employed to calculate the modal loss factor in the objective function. The SIMP interpolation scheme is used in the topology optimization and the sensitivity of the objective function to design variable is further derived. Then, the optimization problem is solved by MMA algorithm.

2. Finite element modeling

2.1. Model description

Figure 1(a) shows a schematic drawing of an element for PCLD patch. h_1, h_2, and t are the thicknesses of the base plate, constraining layer and viscoelastic layer, respectively. In conventional FE model, the base layer and constraining layer are modeled with shell elements and the viscoelastic layer is modeled with three-dimensional solid elements. The coupling between the shell elements and the solid elements are handled by kinematic constraints. The procedure of the solution is very time consuming. In this section, a more efficient model is introduced. The viscoelastic layer is modeled using a special interface element with eight nodes (shown in Fig. 1(b)) that can couples the two stiff layers together directly.

2.2. Modeling of the cover layers

The base layer and the constraining layer of Fig. 1(a) can be meshed with the rectangular nonconforming plate bending element. Based on the classical plate and finite element theory, the displacement field of the element can be written as [26]

$$\{u\} = [H][N]\{u_e\} \tag{1}$$

where

$$[H] = \begin{bmatrix} 1 & 0 & 0 & -z & 0 \\ 0 & 1 & 0 & 0 & -z \\ 0 & 0 & 1 & 0 & 0 \end{bmatrix} \tag{2}$$

$$[N] = \begin{bmatrix} N_1 & N_2 & N_3 & N_4 \end{bmatrix} \tag{3}$$

$$[N_i] = \begin{bmatrix} \psi_i & 0 & 0 & 0 & 0 \\ 0 & \psi_i & 0 & 0 & 0 \\ 0 & 0 & g_{i1} & g_{i2} & g_{i3} \\ 0 & 0 & \partial g_{i1}/\partial x & \partial g_{i2}/\partial x & \partial g_{i3}/\partial x \\ 0 & 0 & \partial g_{i1}/\partial y & \partial g_{i2}/\partial y & \partial g_{i3}/\partial y \end{bmatrix} \tag{4}$$

$\psi_i (i = 1, 2, 3, 4)$ and $g_{ij} (j = 1, 2, 3)$ are the linear and non-conforming Hermite cubic interpolation functions, respectively, which can be expressed as

$$\psi_i = \frac{1}{4}(1 + \xi\xi_i)(1 + \eta\eta_i) \tag{5}$$

$$g_{i1} = \frac{1}{8}(1 + \xi\xi_i)(1 + \eta\eta_i)(2 + \xi\xi_i + \eta\eta_i - \xi^2 - \eta^2) \tag{6}$$

$$g_{i2} = \frac{1}{8}\xi_i(1 + \xi\xi_i)^2(\xi\xi_i - 1)(1 + \eta\eta_i)a \tag{7}$$

$$g_{i3} = \frac{1}{8}\eta_i(1 + \eta\eta_i)^2(\eta\eta_i - 1)(1 + \xi\xi_i)b \tag{8}$$

where a and b are the half lengths of the rectangular element along the x- and y-directions, respectively. $\{u_e\}$ is the nodal displacement vector in the midplane and each node has three translational and two rotational degrees of freedom.

2.3. Modeling of the viscoelastic layer

Shearing is assumed to be the only significant energy storage mechanism in the viscoelastic core, and dissipation under harmonic loading is introduced by taking the core shear modulus to be complex. In a certain frequency range, the shear modulus can be described approximately by a linear and viscoelastic, frequency-independent, complex constant shear modulus as [1,23]

$$G_v^* = G_v(1 + i\eta_v) \tag{9}$$

where G_v is the storage modulus and η_v is the material loss factor. All the displacements are small compared to the structural dimensions thus linear theories of elasticity, viscoelasticity are adopted. Then the displacement field of the thin viscoelastic layer $u^{(2)}$ can be expressed by the displacement field of its surfaces by linear interpolation as

$$\left\{u^{(2)}\right\} = \begin{bmatrix} T_1 & T_2 \end{bmatrix} \left\{ u_b^{(2)} \quad u_t^{(2)} \right\}^T \tag{10}$$

where

$$T_1 = \begin{bmatrix} \frac{1}{2} - \frac{z}{t} & 0 & 0 \\ 0 & \frac{1}{2} - \frac{z}{t} & 0 \\ 0 & 0 & \frac{1}{2} - \frac{z}{t} \end{bmatrix} \tag{11}$$

$$T_2 = \begin{bmatrix} \frac{1}{2} + \frac{z}{t} & 0 & 0 \\ 0 & \frac{1}{2} + \frac{z}{t} & 0 \\ 0 & 0 & \frac{1}{2} + \frac{z}{t} \end{bmatrix} \tag{12}$$

$u_b^{(2)}$ and $u_t^{(2)}$ are the displacement fields of the bottom surface and top surface of the viscoelastic layer, respectively. The superscript T denotes vector transpose. Here, we assume no slip occurs at the interfaces of the layers. Then, the boundary conditions of the viscoelastic layer are given as

$$\left\{ u_b^{(2)} \quad u_t^{(2)} \right\}^T = \left\{ u_t^{(1)} \quad u_b^{(3)} \right\}^T \tag{13}$$

where $u_t^{(1)}$ and $u_b^{(3)}$ are the displacement field of the top surface of the base layer and the bottom surface of the constraining layer, respectively. By introducing Eq. (13) to Eq. (10) and combining Eq. (1), the displacement field of the thin viscoelastic layer is derived as the following equation

$$\left\{ u^{(2)} \right\} = \begin{bmatrix} T_1 & T_2 \end{bmatrix} \begin{bmatrix} H_1 & 0 \\ 0 & H_2 \end{bmatrix} \begin{bmatrix} N & 0 \\ 0 & N \end{bmatrix} \begin{Bmatrix} u_e^{(1)} \\ u_e^{(3)} \end{Bmatrix} \tag{14}$$

where $u_e^{(1)}$ and $u_e^{(3)}$ are nodal displacement vectors of the base layer and constraining layer, respectively. And

$$[H_1] = [H]_{(z=h_1/2)} = \begin{bmatrix} 1 & 0 & 0 & -h_1/2 & 0 \\ 0 & 1 & 0 & 0 & -h_1/2 \\ 0 & 0 & 1 & 0 & 0 \end{bmatrix} \tag{15}$$

$$[H_2] = [H]_{(z=-h_2/2)} = \begin{bmatrix} 1 & 0 & 0 & h_2/2 & 0 \\ 0 & 1 & 0 & 0 & h_2/2 \\ 0 & 0 & 1 & 0 & 0 \end{bmatrix} \tag{16}$$

From Eq. (14), the present interface element directly couples the two cover layers modeled with shell elements to the viscoelastic layer in between with no extra node added. Then, the matrix of elemental interpolation functions is determined and the strain-displacement matrix can be obtained by differentiating the interpolation function matrix with respect to the local element coordinates. Appling the principal of virtual work, the mass matrix and stiffness matrix of the element can be readily calculated.

2.4. Modal loss factor

The main objective in vibration damping is to dissipate the vibration energy, which can be achieved by maximizing the modal loss factors. Based on our FE model, the dynamic equations for free vibration of the structure with viscoelastic materials has the form

$$[M]\ddot{\mathbf{X}} + ([K_R] + j[K_I])\mathbf{X} = 0 \tag{17}$$

where $[M]$ is the global mass matrix, $[K_R]$ is the real part of the global stiffness matrix, $[K_I]$ is the imaginary part of the global stiffness matrix, and $\mathbf{X}$ is the nodal displacement vector. Then, the rth modal loss factor can be found using FE-MSE method as [23]

$$\eta_r = \frac{\phi_r^T [K_I] \phi_r}{\phi_r^T [K_R] \phi_r} \tag{18}$$

where ϕ_r is the rth mode shape vector of the associated undamped system.

2.5. Validation of the finite element model

The calculated natural frequencies and modal loss factors of a sandwich plate from the present model are compared with those from a closed-form solution and also with NASTRAN/MSE predictions published [23], shown in Table 1. The dimensions of the plate is $0.3048\ \mathrm{m} \times 0.348\ \mathrm{m}$, the bottom and top plates have the same thickness of 0.762 mm and the same physical parameters of $E_I = 68.9$ GPa, $v_I = 0.3$, and $\rho_I = 2740$ kg/m^2. The 0.254 mm thick viscoelastic layer has the constant properties of $G_v = 0.896$ MPa, $v_v = 0.49$, $\rho_v = 999$ kg/m^2 and $\eta_v = 0.5$. The boundary conditions are taken as simply supported with unrestrained core shear at edges and 10×12 elements are used in the FE model. The results of the present method have some difference with the analytical results obtained, but still in the acceptable range for engineering applications.

Table 1
Natural frequencies and modal loss factors

Mode	Analytical solution		NASTRAN/MSE		Present model	
	Frequency (Hz)	Loss factor	Frequency (Hz)	Loss factor	Frequency (Hz)	Loss factor
1	60.3	0.190	57.4	0.176	60.7	0.232
2	115.4	0.203	113.2	0.188	113.5	0.213
3	130.6	0.199	129.3	0.188	128.7	0.206
4	178.7	0.181	179.3	0.153	175.4	0.187
5	195.7	0.174	196.0	0.153	193.6	0.180

3. Topology optimization of passive constrained layer damping

3.1. SIMP interpolation scheme

Continuum topology optimization is essentially the integer programming problem with large scale of the 0–1 discrete design variables. However, the optimization problem with large scale of discretized design variables is generally ill-posed and difficult to solve directly using general mathematical programming approaches. Therefore, the 0–1 integer optimization problem is usually relaxed by introducing continuum-type design variables. Two typical approaches are homogenization-based approaches [27] and variable density methods [20]. In our present study, the SIMP is used as interpolation schemes of variable density methods. Define the relative density as the design variable vector

$$\rho = \{\rho_1, \rho_2, \cdots, \rho_{Ne}\} \tag{19}$$

where N_e denotes the total number of the elements. The design domain contains not only viscoelastic layer but also its corresponding constraining layer. Then, the SIMP model can be expressed as

$$[K] = [K^{(1)}] + \sum_{x=1}^{N_e} \rho_x^p([k_x^{(2)}] + j\eta_v[k_x^{(2)}] + [k_x^{(3)}]) \tag{20}$$

$$[M] = [M^{(1)}] + \sum_{x=1}^{N_e} \rho_x^q([m_x^{(2)}] + [m_x^{(3)}]) \tag{21}$$

where $[K^{(1)}]$ and $[M^{(1)}]$ are the stiffness matrix and mass matrix of the base layer, $[k_x^{(2)}]$ and $[m_x^{(2)}]$ are the real part of the stiffness matrix and mass matrix of the xth element of viscoelastic layer, respectively, and $[k_x^{(3)}]$ and $[m_x^{(3)}]$ are the real part of the stiffness matrix and mass matrix of the xth element of constraining layer, respectively. p and q are the penalization factors. These penalty factors are used to accelerate the convergence of iteration results and obtain a clear pattern of the PCLD treatment on the plate. Then, the real part and imaginary part of the global stiffness matrix can be written as

$$[K_R] = [K^{(1)}] + \sum_{x=1}^{N_e} \rho_x^p([k_x^{(2)}] + [k_x^{(3)}]) \tag{22}$$

$$[K_I] = \eta_v \sum_{x=1}^{N_e} \rho_x^p[k_x^{(2)}] \tag{23}$$

3.2. Optimization formulation

For convenience, the objective function is selected as the inverse of the modal loss factor, which transforms the maximum problem to a minimum problem. Furthermore, in order to get an averaged effect over multi-mode, we define the final objective function J as

$$J = \sum_r a_r/\eta_r \tag{24}$$

where a_r is the associated weighting factor and $\sum_r a_r = 1$.

In addition, the constraint should be considered to limit the consumption of PCLD treatments, thus the volume fraction is limited here. Then the mathematical formulation of the optimization problem is defined as

$$\begin{aligned} &\text{Find}: \quad \rho_x, x = 1, 2, \ldots, N_e \\ &\text{Minimization}: \quad J = \sum_r a_r/\eta_r \end{aligned} \tag{25}$$

$$\text{Subject to}: \quad \begin{cases} \sum\limits_{x=1}^{N_e} \rho_x V_x - \alpha V_0 \leqslant 0 \\ (K_r - \lambda_r M)\phi_r = 0 \\ 0 \leqslant \rho_{\min} \leqslant \rho_x \leqslant 1, \quad x = 1, 2, \ldots, N_e \end{cases}$$

where V_x and V_0 are the volume of the element x and the admissible design domain, respectively. α is the maximum total fraction of PCLD coverage. λ_r is the rth eigenvalue of the associated undamped system. The minimum density factor $\rho_{\min}$ is introduced here to avoid numerical problems when calculating the inverse of the stiffness matrix. $\rho_x = \rho_{\min}$ implies no material in the element and $\rho_x = 1$ means the element fully consists of the materials.

3.3. Sensitivity analysis

A key step in solving the topology optimization problem is the sensitivity analysis. Here, the sensitivity of $1/\eta_r$ with respect to the design variable ρ_x is given from Eq. (18) by

$$\frac{\partial}{\partial \rho_x}\left(\frac{1}{\eta_r}\right) = \frac{\left[\dfrac{\partial(\phi_r^T[K_R]\phi_r)}{\partial \rho_x}\right](\phi_r^T[K_I]\phi_r) - \left[\dfrac{\partial(\phi_r^T[K_I]\phi_r)}{\partial \rho_x}\right](\phi_r^T[K_R]\phi_r)}{(\phi_r^T[K_I]\phi_r)^2} \tag{26}$$

Here, for convenience, orthonormal modes are used. That is

$$\phi_r^T[M]\phi_r = 1 \tag{27}$$

Thus, Eq. (26) can be rewritten as

$$\frac{\partial}{\partial \rho_x}\left(\frac{1}{\eta_r}\right) = \frac{\dfrac{\partial \lambda_r}{\partial \rho_x}(\phi_r^T[K_I]\phi_r) - \lambda_r[2\left(\dfrac{\partial \phi_r}{\partial \rho_x}\right)^T K_I\phi_r + \phi_r^T\dfrac{\partial[K_I]}{\partial \rho_x}\phi_r]}{(\phi_r^T[K_I]\phi_r)^2} \tag{28}$$

Following Wang [28], the eigenvalue and eigenvector derivatives are, respectively

$$\frac{\partial \lambda_r}{\partial \rho_x} = \phi_r^T\left(\frac{\partial[K_R]}{\partial \rho_x} - \lambda_r\frac{\partial[M]}{\partial \rho_x}\right)\phi_r \tag{29}$$

$$\frac{\partial \phi_r}{\partial \rho_x} \approx \sum_{i=1}^{\hat{N}} c_i\phi_i + y_r - b_r \tag{30}$$

where

$$c_r = -\frac{1}{2}\phi_r^T \frac{\partial [M]}{\partial \rho_x}\phi_r \tag{31}$$

$$c_i = -\frac{\phi_i^T \frac{\partial [Z_r]}{\partial \rho_x}\phi_r}{\lambda_i - \lambda_r} \quad (i \neq r) \tag{32}$$

$$y_r = [K_R]^{-1} F_r \tag{33}$$

$$b_r = \sum_{i=1}^{\hat{N}} \frac{\phi_i^T F_r \phi_i}{\lambda_i} \tag{34}$$

$$[Z_r] = [K_R] - \lambda_r [M] \tag{35}$$

$$F_r = -\left(\frac{\partial [K_R]}{\partial \rho_x} - \frac{\partial \lambda_r}{\partial \rho_x}[M] - \lambda_r \frac{\partial [M]}{\partial \rho_x}\right)\phi_r \tag{36}$$

and the sensitivities of the mass matrix and real part stiffness matrix can be easily derived from Eqs (21) and (22), respectively.

3.4. Solution method

There are two typical approaches used to solve topological optimization problems: Optimality criteria method (OC) [27] and mathematical programming method. The OC method has been successfully applied to structural topology optimizations, and it is efficient for solving problems with large number of design variables and a few constraints. However, it is hard to construct the explicitly expressed heuristic updating schemes for non-convex and complicated objectives. While the mathematical programming method, e.g. sequential linear programming (SLP), sequential quadratic programming (SQP), and MMA, is usually more flexible and theoretically well founded to deal with advanced topology optimization design with complicated objectives and multiple constraints. In this paper MMA algorithm is introduced to the optimization problem. For more details on this algorithm, see Svanberg's works [21].

3.5. Parameters selection

Theoretically, a more preferable penalizing effect in the SIMP model will be obtained when p has a large value. But we should emphasize that the global stiffness matrix for the FE subroutines will evolve to be singular when $p \geqslant 6$ due to that $\rho_{\min}$ is usually very small. Thus the reasonable range of SIMP exponent for engineering application should be within $3 \leqslant p \leqslant 5$. In this paper, a typical value $p = 3$ is used. Then the relaxed optimization problem can approximately approach the original optimization problem with 0–1 design variables in a weak form, and the effect of those stiffness matrixes, corresponding to intermediate densities' elements penalized by p, upon global stiffness matrix can be reasonably ignored.

In the procedure of the topology optimization, there is a big difference in the stiffness and mass of the void and solid elements, which has the possibility to generate pseudo modes. The objective function of the present study is highly related to the eigenvalues and the eigenvectors, so the pseudo modes may lead to erroneous results. The desired solutions can be obtained by removing the elements from the finite element model when they become void. However, this is not feasible in topology optimization because once the element has been removed it is not possible for it to come back. We have to work with a finite element model with a mixture of void and solid elements on a fixed grid in the optimization procedure. There are some methods for avoiding pseudo modes, e.g., reinforcement optimization [29], non-structural masses, neglecting low density areas [30]. In the present paper, we mainly concern the low order modes of the structure. A simple and feasible way is to increase the eigenvalues of the local low density area by penalizing the mass matrix more than stiffness matrix. Then the mass of void elements will be small compared with their stiffness, low order pseudo modes will vanish.

Table 2
Comparison of natural frequencies and modal loss factors

Mode	General FEM		$p = 3, q = 1$		$p = 3, q = 2$		$p = 3, q = 3$	
	Freq. (Hz)	loss factor	Freq. (Hz)	loss factor	Freq. (Hz)	loss factor	Freq. (Hz)	loss factor
1	39.9491	0.0922	39.8038	0.092	39.9477	0.0922	39.9492	0.0922
2	80.1654	0.0296	70.6785	0.4117	80.1623	0.0296	80.1655	0.0296
3	103.2073	0.0795	79.8371	0.0298	103.2073	0.0795	103.2074	0.0795
4	140.7306	0.0570	88.4680	0.2628	140.7256	0.0570	140.7307	0.0570
5	155.9559	0.0140	92.9127	0.2382	155.9484	0.0140	155.9561	0.0140

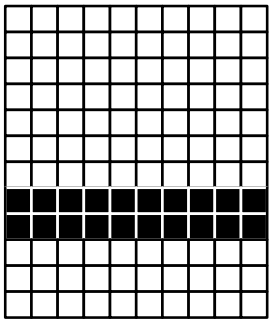

Fig. 2. A clear 0–1 design with PCLD partially covered on plate.

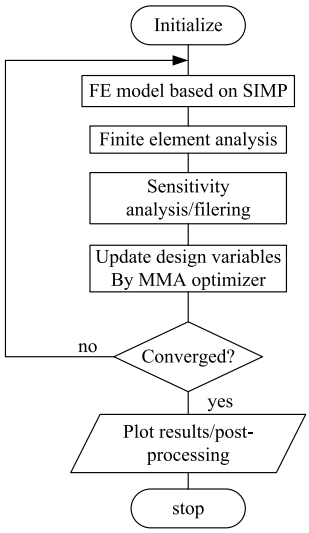

Fig. 3. The scheme of the topology optimization.

Figure 2 shows a clear 0–1 design of PCLD on plate. The parameters of the model are the same as that of the model in Section 2.5, but for PCLD partially covered. Black elements mean there are PCLD covered on the base plate, and white elements mean there are only baseline elements. The first five mode frequencies and loss factors are calculated by the methods of general FEM by removing void elements and the SIMP FE model by setting q to different values with $p = 3$, $\rho_{\min} = 0.01$. The results are compared in Table 2. When $q = 1$, the results of 2^{nd}, 4^{th} and 5^{th} modes are clearly not the results wanted. The mass of the void elements is high compared with their stiffness and then leads to local pseudo modes of the structure in very low frequencies. By increasing the value of q, the situation is improved. When $q = 3$, there are almost no difference in natural frequencies and modal loss factors between the general FEM and the SIMP model. Hence, in our work, we set q to 3 to avoid local pseudo modes.

3.6. Numerical instabilities

When a suitable penalty factor is exerted upon SIMP model, the global stiffness matrix will not be very sensitive to the elements with intermediate density values compared to the elements with solid material. Although SIMP can compress intermediate density effectively, it cannot overcome numerical instabilities such as checkerboards [31] and mesh-dependency [32]. Filtering [33] is always used on the sensitivities of the optimization to overcome the problem. Sensitivity filtering technology is actually a heuristic method which works by substituting the original element sensitivities with a weighted average of the sensitivities around their neighbors within a given characteristic radius. Thus the smooth and differential properties of the sensitivity field are somewhat improved, and the regularized sensitivities are obtained by the convolution of a compact linear operator with original element sensitivities. Consequently, the objective smoothness of the optimization problem is enhanced to some extent, and the gradient filter method is seemingly efficient to prevent the checkerboards and the mesh-dependences in engineering applications. With this method, the topology optimization problem with relaxation will become well-posed without checkerboards

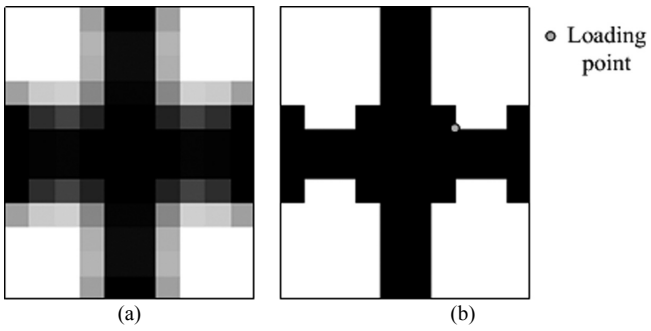

Fig. 4. Optimized topology of PCLD treatment on the rectangular plate. (a) before post-processing; (b) after post-processing.

and mesh-dependency. The continuum-type optimal solution would approximate the original optimization problem with 0–1 design variables. In this work, the sensitivity filtering approach is introduced. The applied details can refer to Sigmund's work [33].

4. Optimization scheme

According to the above analysis, the topology optimization scheme based on the SIMP model is represented in Fig. 3. The procedure is listed as follows:

Step 1. Make initial design, e.g., mesh the structure, define design domain, constraints, and initialize design variables with a predetermined relative density value.
Step 2. Determine the stiffness and mass matrices using the current design variables based on SIMP model.
Step 3. Calculate the value of the objective function using MSE method.
Step 4. Analysis the sensitivities of objective function. In order to prevent checkerboard patterns in the design, sensitivity filtering is introduced.
Step 5. Update the design variables using the MMA algorithm.
Step 6. Check the convergence of the result. The convergence condition here is that the maximum change of the variables between the current and the last iteration is smaller than 0.005. If the result does not converge, return to step 2. Else continue to step 7.
Step 7. Output the design variables and objective value, plot the results and do post-processing of the results.

5. Numerical results

Two typical plates of different shapes are considered in this section. To evaluate the performance of the optimized result, we apply a unit transverse harmonic point load of 1 N at the loading point on the plate and compare the transverse response at the point with that of bare plate and fully PCLD covered plate.

5.1. Rectangular plate

We consider the case of the rectangular plate discussed in Section 2.5 but for partial coverage. Here, only first three modes are of interest and weighting factors in the objective function are $a_1 = 0.3$, $a_2 = 0.5$ and $a_3 = 0.2$, respectively. The volume fraction is 0.48 as the constraint condition.

Figure 4(a) shows the optimized PCLD layout on the rectangular plate. A 0–1 design, shown in Fig. 4(b), is derived from Fig. 4(a) used a simple post-processing of the results by setting the intermediate density of material to zero when it is smaller than a reference value, and else, setting the density to one. Considering the penalization factor $p = 3$, the reference value is chosen as $\sqrt[3]{0.5}$. Figure 5 shows the development of the objective function along the optimization process. We can see the objective function converges rapidly. The location of the loading point is

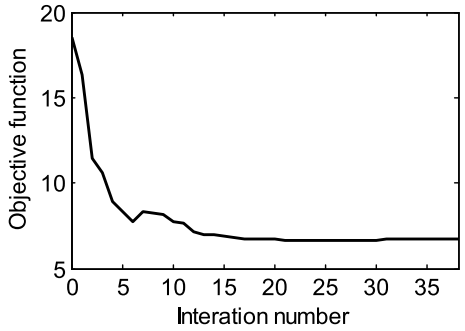

Fig. 5. Convergence history for the rectangular plate.

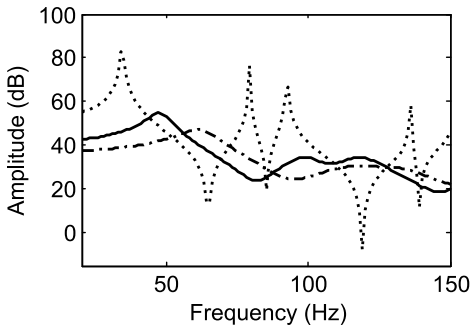

Fig. 6. Displacement amplitude versus frequency at the loading point of the rectangular plate. Dot line represents bare plate, solid line represents plate with optimized PCLD layout and dot-dash line represents plate with PCLD fully covered.

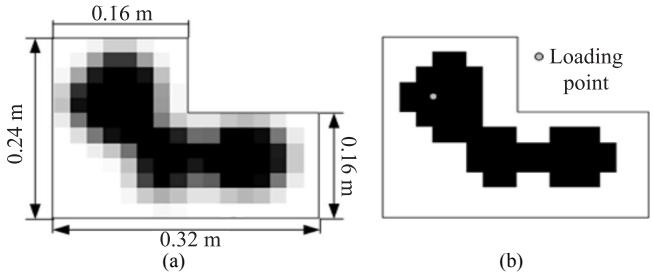

Fig. 7. Optimized topology of PCLD treatment on the "L" shape plate. (a) before post-processing; (b) after post-processing.

selected at the node points offset from the nodal lines for the first three modes of bare plate shown in Fig. 4(b). The frequency responses at the loading point corresponding to different cases are illustrated in Fig. 6. It can be seen that the results of the partial coverage case are not as good as that of the full coverage case, but they still have significant improvement comparing with the results of the bare plate, and have 60% weight of the PCLD patch saved comparing with the full coverage case.

5.2. "L" shape plate

A nonsymmetrical plate with "L" shape is studied here as it is a typical shape for industrial and realistic application, e.g., an oil pan or a front cover of the engine of a car. The plate is made of the same Aluminum material as in the foregoing example and its thickness is 2 mm. The dimensions are shown in Fig. 7(a). The boundary conditions are taken as clamped at all edges. The PCLD patch consists of a 0.8 mm thick Aluminum sheet and a 0.25 mm thick viscoelastic layer. The constant properties of the viscoelastic layer are $G_v = 8.6$ MPa, $v_v = 0.49$, $\rho_v = 1300$ kg/m^2 and $\eta_v = 0.5$. First three modes are concerned and $a_1 = 0.3$, $a_2 = 0.4$ and $a_3 = 0.3$. The volume fraction is set to 0.4.

The optimized distribution of the PCLD patch on the "L" shape plate as a result of topology optimization is shown in Fig. 7(a). Figure 7(b) shows the 0–1 design derived from Fig. 7(a) by the post-processing described above. The convergent history is shown in Fig. 8. The objective function decreases smoothly and rapidly with the iteration number increase until the convergence condition is satisfied. Figure 9 shows the frequency responses at the loading point illustrated as Fig. 7(b) corresponding to three different cases. It is very promising to see that the optimized partial coverage case has almost the same damping effect as that of the full coverage case for suppressing the plate vibration with more than 68% weight saved.

Furthermore, it should be noted that there are resonant frequencies' shifts in Fig. 6 and Fig. 9, when the PCLD treatments are patched on the base plate. From the aspect of structural frequency response, the shifts caused by the additional stiffness of the constraining layer should not be deviated from the original one too far away. It can be seen that the optimized partially covered cases provide smaller shifts than the fully covered cases. When the base plate

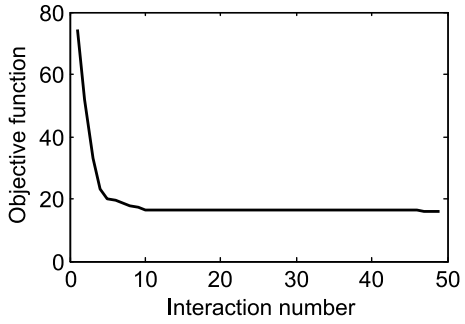

Fig. 8. Convergence history for the "L" shape plate.

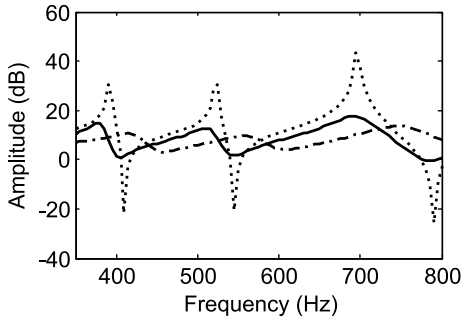

Fig. 9. Displacement amplitude versus frequency at the loading point of the "L" shape plate. Dot line represents bare plate, solid line represents plate with optimized PCLD layout and dot-dash line represents plate with PCLD fully covered.

is much stiffer than the constraining layer and the coverage of the PCLD patch is small, the frequency shifts are not very obvious as we can see from Fig. 9 for the partially covered case. If the effect of the frequency shifts can't be ignore, we should add a penalty function about the frequencies' shift in the objective function as discussed by Chen and Huang [34].

6. Conclusion

This paper has presented a topology optimization approach to optimally design of PCLD treatments on plates. In the proposed approach, an interface finite element is introduced to modeling the viscoelastic layer of PCLD treatment to simplify the FE model in the optimization procedure. The SIMP interpolation scheme is applied to generate the mass and stiffness matrices of the structure and the penalization factors are well selected to avoid local pseudo modes. The optimization problems are solved by MMA algorithm. Then, numerical results are presented for two typical shape plates. It's found that the objective function is in a steady convergence process and the optimized PCLD layouts have very high damping characteristics and are also very light in weight. The proposed approach can be an important design tool for flat plates with PCLD treatments in order to enhance energy dissipation and suppress structural vibration in an economical and effective way.

It is worth to point out that the work presented in this paper is limited to the case where the property of viscoelastic material is frequency-independent. It is, therefore, meaningful to carry out further study targeting to other frequency-dependent objective functions, e.g., minimizing the structural response, minimizing the radiated sound power, when the property of viscoelastic material is frequency-dependent. Furthermore, the base structure is limited to the flat plat. Thus, one more meaningful work is to extend the application of the proposed approach to arbitrary shape thin-walled structures. The third, the resonance frequency shift should be considered in the objective function in future study.

Acknowledgments

Supported by the National Basic Research Program of China (973 Program) (Grant No. 2010CB736100), the National Science Foundation of China (Grant No. 51175195) and the China Postdoctoral Science Foundation Funded Project (Grant No. 2012M511608).

References

[1] B.C. Nakra, Vibration control in machines and structures using viscoelastic damping, *Journal of Sound Vibration* **211** (1998), 449–465.

[2] E.M. Kerwin, Damping of flexural waves by a constrained viscoelastic layer, *Journal of the Acoustical Society of America* **32** (1959), 952–962.
[3] R.A. DiTaranto, Theory of vibratory bending for elastic and viscoelastic layered finite-length beams, *ASME Journal of Applied Mechanics* **32** (1965), 881–886.
[4] D.J. Mead and S. Markus, The forced vibration of a three-layer, damped sandwich beam with arbitrary boundary conditions, *Journal of Sound Vibration* **10** (1969), 163–75.
[5] M.D. Rao and S. He, Dynamic analysis and design of laminated composite beams with multiple damping layers, *AIAA Journal* **31** (1993), 736–745.
[6] A. Baz, Robust control of active constrained layer damping, *Journal of Sound Vibration* **211** (1998), 467–480.
[7] I.Y. Shen, Hybrid damping through intelligent constrained layer treatments, *ASME Journal of Vibration and Acoustics* **116** (1994), 341–349.
[8] R. Plunkett and C.T. Lee, Length optimization of constrained viscoelastic layer damping, *Journal of the Acoustical Society of America* **48** (1970), 150–161.
[9] A.K. Lall, B.C. Nakra and N.T. Asnani, Optimum design of viscoelastically damped sandwich panels, *Engineering Optimization* **6** (1983), 197–205.
[10] J.L. Marcelin, Ph. Trompette and A. Smati, Optimal constrained layer damping with partial coverage, *Finite Elements in Analysis and Design* **12** (1992), 273–280.
[11] H. Zheng, C. Cai and X.M. Tan, Optimization of partial constrained layer damping treatment for vibration energy minimization of vibrating beams, *Computers and Structures* **82** (2004), 2493–2507.
[12] H. Zheng and C. Cai, Minimization of sound radiation from baffled beams through optimization of partial constrained layer damping treatment, *Applied Acoustics* **65** (2004), 501–520.
[13] M. Alvelid, Optimal position and shape of applied damping material, *Journal of Sound and Vibration* **310** (2008), 739–756.
[14] M.P. Bendsøe and N. Kikuchi, Generating optimal topologies in structural design using a homogenization method, *Computer Methods in Applied Mechanics and Engineering* **71** (1988), 197–224.
[15] G.I.N. Rozvany, A critical review of established methods of structural topology optimization, *Structural and Multidisciplinary Optimization* **37** (2009), 217–237.
[16] Y.M. Yi, S.H. Park and S.K. Youn, Design of microstructures of viscoelastic composites for optimal characteristics, *International Journal of Solids and Structures* **37** (2000), 4791–4810.
[17] A. Lumsdaine, Topology optimization of constrained damping layers treatments, *ASME 2002 International Mechanical Engineering Congress and Exposition*, IMECE2002-39021, 149–156.
[18] A. Al-Ajmi Mohammed, Homogenization and structural topology optimization of constrained layer damping treatments, Ph. D Dissertation, *University of Maryland*, 2004.
[19] Z. Ling, X. Ronglu, W. Yi and A. El-Sabbagh, Topology optimization of constrained layer damping on plates using method of moving asymptote(MMA) approach, *Shock and Vibration* **18** (2011), 221–244.
[20] M.P. Bendsøe and O. Sigmund, Material interpolations in topology optimization, *Archive of Applied Mechanics* **69** (1999), 635–654.
[21] K. Svanberg, The method of moving asymptotes-a new method for structural optimization, *International Journal for Numerical Methods in Engineering* **24** (1987), 359–373.
[22] Y.P. Lu, J.W. Killian and G.C. Everstine, Vibrations of three layered damped sandwich plate composites, *Journal of Sound and Vibration* **64** (1979), 63–71.
[23] C.D. Johnson and D. Kienholz, Finite element prediction of damping in structures with constrained viscoelastic layers, *AIAA Journal* **20** (1981), 1284–1290.
[24] Q.J. Zhang and M.G. Sainsbury, The galerkin element method applied to the vibration of rectangular damped sandwich plates, *Computers and Structures* **74** (2000), 717–730.
[25] M. Alvelid and M. Enelund, Modelling of constrained thin rubber layer with emphasis on damping, *Journal of Sound and Vibration* **300** (2007), 662–675.
[26] K.Y. Lam, X.Q. Peng, G.R. Liu and J.N. Reddy, A finite-element model for piezoelectric composite laminates, *Smart Materials and Structures* **6** (1997), 583–591.
[27] B. Hassani and E. Hinton, A review of homogenization and topology optimization-topology optimization using optimality criteria, *Computers and Structures* **69** (1998) 739–756.
[28] B.P. Wang, Improved approximate methods for computing eigenvector derivatives in structural dynamics, *AIAA Journal* **29** (1990), 1018–1020.
[29] L.H. Tenek and I. Hagiwara, Static and vibrating shape and topology optimization using homogenization and material programming, *Computer Methods in Applied Mechanics and Engineering* **109** (1993), 143–154.
[30] N.L. Pederson, Maximization of eigenvalues using topology optimization, *Structural and Multidisciplinary Optimization* **20** (2000), 2–11.
[31] A. R. Diaz and O. Sigmund, Checkerboard patterns in layout optimization, *Structural and Multidisciplinary Optimization* **10** (1995), 40–45.
[32] M. Zhou, Y.K. Shyy and H.L. Thoms, Checkerboard and minimum member size control in topology optimization, *Structural and Multidisciplinary Optimization* **21** (2001), 152–158.
[33] O. Sigmund and J. Petersson, Numerical instabilities in topology optimization: A survey on procedures dealing with checkerboards, mesh-dependencies and local minima, *Structural and Multidisciplinary Optimization* **16** (1998), 68–75.
[34] Y.C. Chen and S.C. Huang, An optimal placement of CLD treatment for vibration suppression of plates, *International Journal of Mechanical Science* **44** (2002), 1801–1821.